WATER RESOURCES RESEARCH, VOL. 49, 5778–5791, doi:10.1002/wrcr.20463, 2013

Accuracy of the cosmic-ray soil water content probe in humid forest ecosystems: The worst case scenario

H. R. Bogena,[1] J. A. Huisman,[1] R. Baatz,[1] H.-J. Hendricks Franssen,[1] and H. Vereecken[1]

Received 18 April 2013; revised 25 July 2013; accepted 8 August 2013; published 13 September 2013.

[1] Soil water content is one of the key state variables in the soil-vegetation-atmosphere continuum due to its important role in the exchange of water and energy at the soil surface. A new promising method to measure integral soil water content at the field or small catchment scale is the cosmic-ray probe (CRP). Recent studies of CRP measurements have mainly presented results from test sites located in very dry areas and from agricultural fields with sandy soils. In this study, distributed continuous soil water content measurements from a wireless sensor network (SoilNet) were used to investigate the accuracy of CRP measurements for soil water content determination in a humid forest ecosystem. Such ecosystems are less favorable for CRP applications due to the presence of a litter layer. In addition, lattice water and carbohydrates of soil organic matter and belowground biomass reduce the effective sensor depth and thus were accounted for in the calibration of the CRP. The hydrogen located in the biomass decreased the level of neutron count rates and thus also decreased the sensitivity of the cosmic-ray probe, which in turn resulted in an increase of the measurement uncertainty. This uncertainty was compensated by using longer integration times (e.g., 24 h). For the Wüstebach forest site, the cosmic-ray probe enabled the assessment of integral daily soil water content dynamics with a RMSE of about 0.03 cm^3/cm^3 without explicitly considering the litter layer. By including simulated water contents of the litter layer in the calibration, a better accuracy could be achieved.

Citation: Bogena, H. R., J. A. Huisman, R. Baatz, H.-J. Hendricks Franssen, and H. Vereecken (2013), Accuracy of the cosmic-ray soil water content probe in humid forest ecosystems: The worst case scenario, *Water Resour. Res.*, *49*, 5778–5791, doi:10.1002/wrcr.20463.

1. Introduction

[2] Soil water content is one of the key state variables in the soil-vegetation-atmosphere continuum due to its important role in the exchange of water and energy at the soil surface. Soil water content also impacts crop growth and the fate of agricultural chemicals applied to soils. For improving understanding and modeling of soil hydrological processes, measurements of soil water content are required at multiple spatial and temporal scales [*Vereecken et al*., 2008]. For instance, wireless sensor network technology has recently been used for characterization of soil water content at the small catchment scale (27 ha) with high spatial and temporal resolution [*Bogena et al*., 2010; *Rosenbaum et al*., 2012].

[3] A new and promising method to measure soil water content at the field or small catchment scale is the cosmic-ray probe (CRP) [*Zreda et al*., 2008, 2012] that utilizes the fact that fast neutrons produced by natural nucleonic cosmic-ray radiation show a negative correlation with soil water content near the CRP (~330 m radius). This natural cosmic-ray radiation can be divided in primary cosmic rays that originate from space or the sun and secondary cosmic rays generated by interaction with matter in the atmosphere or the top few meters of the earth's crust. The primary cosmic radiation consists of ~90% protons, ~9% α-particle, and ~1% heavier nuclei. Nearly all primary cosmic rays that reach the earth's atmosphere are from outside the solar system, but from within our galaxy [*Gaisser*, 1990].

[4] Solar cosmic rays are caused by sporadic, individual events, whereas galactic cosmic rays come in permanently. Nevertheless, the amount of galactic cosmic rays that reach the top of earth's atmosphere underlies temporal fluctuations caused by the magnetic field of the heliosphere, the so-called solar modulation. When the sun has many spots, its magnetic field is strong. In this case, the charged primary cosmic-ray particles are deflected, and the cosmic-ray intensity on earth is reduced. In addition, cosmic rays of lower energies are deflected to a stronger degree which leads not only to changes in cosmic-ray intensity but also to a shift in the cosmic-ray energy spectrum [*Parker*, 1965].

[5] The protons making up the primary cosmic-ray flux need to possess enough energy to penetrate the earth's magnetosphere in order to reach earth. The minimum energy needed is determined by the cutoff rigidity (momentum-to-charge ratio) of the geomagnetic field, which generally increases with decreasing latitude [*Desilets and Zreda*, 2001]. The geomagnetic field exerts significant influence

[1]Agrosphere Institute (IBG-3), Forschungszentrum Jülich GmbH, Jülich, Germany.

Corresponding author: H. R. Bogena, Agrosphere Institute (IBG-3), Forschungszentrum Jülich, 52425 Jülich, Germany. (h.bogena@fz-juelich.de)

0043-1397/13/10.1002/wrcr.20463

on the primary cosmic-ray flux on top of the atmosphere, because the geomagnetic field extends beyond the atmosphere. Primary cosmic-ray particles that penetrate the atmosphere collide with atmospheric nuclei, generating a nucleonic cascade of secondary cosmic-ray particles that consists mainly of neutrons [*Lal and Peters*, 1967]. These neutrons are produced by two kinds of interactions. In the first type of interaction, knockout neutrons are directly knocked out of a nucleus by an incoming proton or neutron, and they possess energies of ~1 MeV up to the energy of the incoming particle. In the second type of interaction, evaporation neutrons are generated by a deexcitation reaction of the initially excited nuclei of nitrogen and oxygen. These secondary neutrons have a median energy of about 1–2 MeV [*Hess et al*., 1961; *Hendrick and Edge*, 1966] and are further moderated by collisions with nuclei producing neutrons of progressively lower energies (i.e., low-energy thermal (0.025 eV) and epithermal (>0.5 eV) neutrons). Therefore, a pool of neutrons of lower energies is produced. At sufficiently low energies, neutrons are absorbed and thus removed from this pool [*Phillips et al*., 2001].

[6] Since collisions with small nuclei transfer most energy, hydrogen is by far the best neutron moderator [*Zreda et al*., 2012]. Hydrogen atoms in the soil, which are mainly present as water, moderate the secondary neutrons on their way back to the surface. Therefore, fewer neutrons reach the surface in moist soils, whereas under drier conditions more neutrons are able to escape from soil. This fact enables the use of the CRP to sense soil water content. However, the neutron count rates as well as the sensing volume of the CRP depend on the total amount of hydrogen within the sensor footprint and not only on the hydrogen contained in soil water [*Zreda et al*., 2012]. Additional sources of hydrogen are present in different compartments, such as aboveground and belowground biomass, humidity of the lower atmosphere, lattice water of the soil minerals, litter layer, intercepted water in the canopy, and soil organic matter. In the case that the amount of hydrogen within these compartments shows temporal variations, this variation has to be considered in order to determine soil water content dynamics using CRP measurements.

[7] Studies evaluating the use of CRP measurements for soil water content sensing have been restricted to high altitudes (Mt. Lemmon Cosmic Ray Laboratory, Arizona, at 2745 m above sea level (asl), and Lewis Springs, Arizona, at 1233 m asl), coastal sites on Hawaii [*Desilets et al*., 2010], a site within a desert area in Arizona, USA [*Franz et al*., 2012b], and a site within an agricultural field with sandy soils and relatively low soil water content in Germany [*Rivera Villarreyes et al*., 2011]. Because of the high altitude and/or low soil water content, these three test sites had rather favorable conditions for soil water content sensing with the CRP. Since the CRP measures all hydrogen present in its footprint, other hydrogen pools besides soil water content will reduce the sensitivity of the sensor to soil water content changes. To our knowledge, only limited or preliminary assessments of CRP data have been presented up to now in less favorable sites (e.g., low altitude, high mean soil water content, and dynamic changes in hydrogen content of other compartments besides soil water).

[8] Within this context, the main objective of this study is to evaluate the accuracy of CRP measurements for soil water content determination in a low-altitude humid forested catchment using a wireless soil water content sensor network. In order to achieve this, we have (i) investigated the relative importance of lattice water, soil organic matter, and belowground biomass for the effective sensor depth in forest soils; (ii) determined the contribution of different hydrogen pools to the total hydrogen present in the CRP footprint for our forest site; (iii) developed a vertical weighting function that accounts for all important hydrogen pools typically present in humid forest ecosystems and enables the comparison of the sensor network data with the water content estimates of the CRP; (iv) investigated the uncertainty of CRP measurements for different soil water contents and integration times; and (v) considered the time-variable water content of the litter layer in the calibration of the CRP.

2. Materials and Methods

2.1. The Wüstebach Test Site

[9] This study was undertaken in the Wüstebach test site, which is a small subcatchment of the Rur catchment and part of the TERENO Eifel/Lower Rhine Valley Observatory [*Zacharias et al*., 2011] located in the German low mountain ranges within the National Park Eifel (50°30′N, 6°19′E) near the German-Belgian border (see Figure 1).

[10] The Wüstebach test site covers an area of ~27 ha, with altitudes ranging from 595 m asl in the northern part to 628 m asl in the south. The average slope is 3.6% and the maximum slope is 10.4%. The geology is dominated by Devonian shales with occasional sandstone inclusions, which is covered by a periglacial solifluction layer of about 1–2 m thickness. Cambisols and planosols have developed on the hillslopes, whereas gleysols and half-bogs have formed under the influence of groundwater in the valley (Figure 1). The main soil texture is silty clay loam with a medium to high fraction of coarse material, and the litter layer has a thickness between 3 and 5 cm [*Richter*, 2008]. The mean annual precipitation at the test site is 1220 mm for the period 1979–1999 [*Bogena et al*., 2010]. Norway spruce (*Picea abis* L.) planted in 1946 is the prevailing vegetation type (~90%) [*Etmann*, 2009].

2.2. The Wireless Sensor Network SoilNet

[11] SoilNet is a wireless sensor network developed at the Forschungszentrum Jülich. It enables the measurement of soil water content pattern dynamics in small catchments up to several square kilometers [*Bogena et al*., 2010]. Wireless sensor networks have the advantage that the sensors remain in the exact same position, so that the measured values are not affected by small-scale spatial variability of the soil, in contrast to measurements from field campaigns. SoilNet uses the license-free protocol stack JenNet, based on IEEE 802.15.4 (250 kbit/s) specifications, for short-range wireless network applications [*Bogena et al*., 2010]. The SoilNet system consists of one coordinator and several routers and sensor units. The coordinator enables the long-distance data transmission of the measured values (e.g., via GSM modem) and initiates the wireless links within the

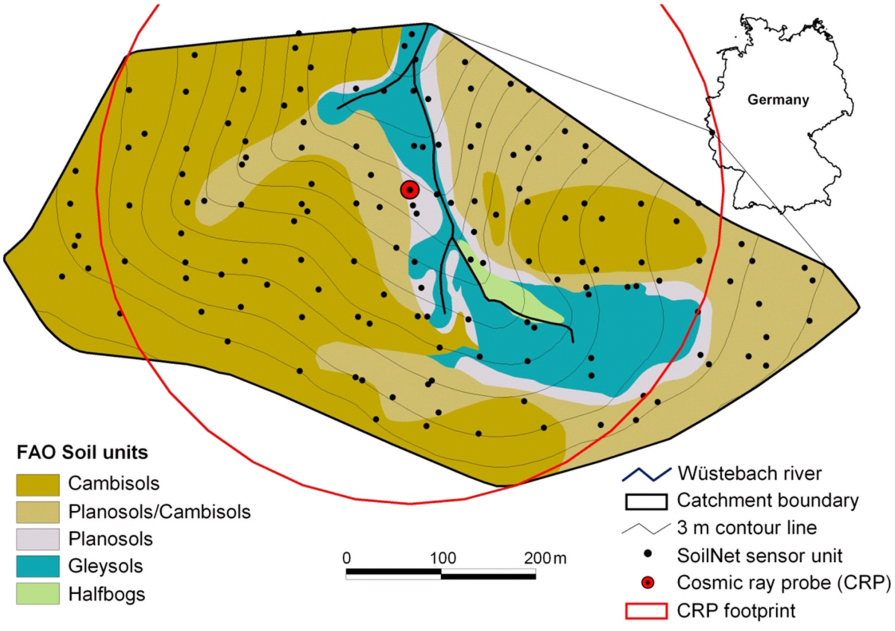

Figure 1. Location of the Wüstebach experimental test site.

network. The sensor units are deployed in the soil, measure the soil water content, and transmit the data to the nearest router.

[12] For the SoilNet application in the Wüstebach catchment, ECH2O EC-5, and ECH2O 5TE sensors (Decagon Devices, Pullman, WA, USA) were used, which have been evaluated by *Rosenbaum et al*. [2010]. The sensors were calibrated following the procedure described in *Rosenbaum et al*. [2012]. The SoilNet in Wüstebach consists of 150 sensor units with 600 ECH2O EC-5 and 300 ECH2O 5TE sensors buried at three depths (5, 20, and 50 cm). There are two sensors at each depth that measure soil water content every 15 min.

2.3. The Cosmic-Ray Soil Water Content Probe

[13] We used the CRS-1000 cosmic-ray soil moisture probe (Hydroinnova LLC, Albuquerque, NM, USA) that measures neutron counts at hourly interval. The main system components are two detector tubes, two pulse modules, and sensors for temperature, atmospheric pressure, and relative humidity. Unshielded detector tubes respond mainly to neutrons in the thermal energy range. In order to detect neutrons in the fast energy range, one detector tube is shielded with polyethylene that moderates fast neutrons to thermal neutrons before they enter the detector tube. The tubes are filled with ^{3}He, which has a high neutron absorption cross section. A potential of $\sim$1000V is applied between the tube wall (cathode) and a thin wire in the center of the tube (anode). Neutrons that enter the tube and hit a ^{3}He atom produce electrons that are deposited on the anode. They induce a pulse of electrical current that is send to the pulse module, which amplifies, detects, and counts these current pulses. The number of counts per hour is sent to the data logger and then to a remote desktop using an integrated modem [*Zreda et al*., 2012].

[14] The cosmic-ray probe was mounted on a pole (50°30′12.38″N, 6°19′59.32″E, WGS84) about 1.2 m above the ground (see Figure 2). Precipitation and atmospheric pressure were measured hourly at the nearby climate station Kalterherberg operated by the German Weather Service. The measurement period that is analyzed here started on 1 February 2011 and ended on 31 December 2012.

Figure 2. The cosmic-ray probe located in the Wüstebach test site.

2.4. Neutron Count Corrections

[15] Since the cosmic-ray flux is exponentially attenuated as a function of the traversed cumulative mass, changes in atmospheric pressure cause relatively large changes in neutron count rate. Therefore, neutron count rates are normalized to standard atmospheric pressure using

$$N_p = N_{raw} \cdot e^{\left(\frac{P-P_0}{L}\right)} \quad (1)$$

where N_p is the corrected count rate, N_{raw} is the raw count rate, P_0 is a reference atmospheric pressure (1013.25 hPa), and P is the actual air pressure. L denotes the mass attenuation length for high-energy neutrons and depends on latitude [*Desilets and Zreda*, 2003]. For the Wüstebach test site, a value of 131.6 g/cm^2 was chosen.

[16] Since the CRP utilizes the natural cosmic-ray neutron flux, the obtained count rates also need to be corrected for variations in the incoming neutron flux. Data from neutron monitors were used to correct for such deviations using the following correction function:

$$N_{pi} = N_p \cdot \frac{N_{avg}}{N_{nm}} \quad (2)$$

where N_{pi} is the neutron count rate corrected for variations in incoming cosmic-ray flux, N_{nm} is the current neutron monitor count rate, and N_{avg} is the neutron monitor count rate averaged over the investigation period. Freely available neutron monitor data from the stations Kiel and Jungfraujoch were averaged and used for the correction (www.nmdb.eu).

[17] In a third step, we accounted for atmospheric water vapor fluctuations using the approach of *Rosolem et al*. [2013]:

$$N_{pih} = N_{pi} \cdot \left(1 + 0.0054 \cdot \left(p_{v0} - p_{v0}^{ref}\right)\right) \quad (3)$$

in which N_{pih} is the neutron count rate corrected for variations in water vapor, and p_{v0} and p_{v0}^{ref} are the absolute humidity (kg/m^3) at the time of measurement and at the reference time. In addition to these corrections, the measured neutron counts were corrected for obvious outliers due to technical issues by removing count rates lower than 350 and higher than 2000 counts/h.

2.5. Calibration of the CRP

[18] According to *Desilets et al*. [2010], the count rate can be related to soil water content by

$$\theta_v = (a_0 \cdot \rho_{bd})\left(\frac{N_{pih}}{N_0} - a_1\right)^{-1} - (a_2 \cdot \rho_{bd}) \quad (4)$$

where θ_v is the volumetric soil water content (cm^3/cm^3), N_0 is the count rate over dry soil under the same reference conditions, and a_i are fitting parameters ($a_0 = 0.0808$, $a_1 = 0.372$ and $a_2 = 0.115$ for values of $\theta > 0.02$ kg/kg). The parameters a_0 and a_2 are multiplied by the dry soil bulk density ρ_{bd} (g/cm^3) to convert the gravimetric soil water content obtained from the original equation by *Desilets et al*. [2010] to volumetric water content. Equation (4) is solved for N_0 using θ_v determined from in situ soil water content measurements within the CRP footprint and measured N_{pih}. Using MCNPx simulations for generic silica soils, *Desilets et al*. [2010] derived the following fitting parameters: $a_0 = 0.0808$, $a_1 = 0.372$, and $a_2 = 0.115$ for values of $\theta > 0.02$ kg/kg.

2.6. Quantification of Belowground Hydrogen Pools Within the CRP Footprint

[19] Belowground hydrogen pools influence the sensing depth of the cosmic-ray sensor and thus have to be considered for proper interpretation of CRP measurements [*Franz et al*., 2012a]. The following belowground hydrogen pools were considered in addition to hydrogen in soil pore water: lattice water, organic matter, and root biomass. The hydrogen content in these pools was assumed to be constant over the duration of this study. To account for these pools, the total belowground hydrogen pool H_p was expressed in g H_2O per cm^3 of soil as follows:

$$H_p = LW + SOM + RB + \rho_w \theta_v \quad (5)$$

in which ρ_w is the density of liquid water (g/cm^3), LW denotes g H_2O in lattice water per cm^3 of soil in the mineral grains and bound water, SOM denotes g H_2O in organic matter per cm^3 of soil, and RB denotes g H_2O in the root biomass per cm^3 of soil. As suggested by *Franz et al*. [2013], the weight of SOM and RB was converted to an equivalent amount of water by assuming that the organic matter consists mainly of cellulose. More detailed information on the determination of LW and SOM can be found in *Franz et al*. [2013]. Hydrogen in the root biomass was estimated following *Gregory* [2006].

[20] For the determination of the belowground hydrogen pools, we collected 108 soil cores from 18 locations within the CRP footprint (6 directions at 25, 75, and 175 m distance from the CRP) using a Humax soil corer. These distances were obtained from the sampling scheme suggested by the COSMOS (Cosmic-ray Soil Moisture Observing System) project [*Zreda et al*., 2012] and were selected so that a simple arithmetic average of the samples represents the CRP footprint. The length of each core was 30 cm and the volume was ~39 cm^3. Each core was divided in six samples of 5 cm length, and these samples were analyzed for seven soil properties (see Table 1). The bulk density was derived using the oven drying method (105°C for 48 h). Subsequently, the soil samples were sieved and merged to generate a mixed sample for each depth. From these bulked samples, three 15 mg aliquots were taken and burned at 1000°C. For lattice water determination, hydrogen atoms were detected using a heat conductivity detector. The total organic carbon was detected using a VARIO EL Cube (Elementar Analysensysteme GmbH).

2.7. Determination of the CRP Sensing Volume

[21] The horizontal footprint has a radius of about 330 m and is almost independent of soil water content [*Zreda et al*., 2008; *Desilets and Zreda*, 2013]. In contrast, the measurement depth is strongly dependent on soil water content (~75 cm for dry soils and ~12 cm for wet soils). The effective measurement depth, z^*, can be expressed as [*Franz et al*., 2012a]

Table 1. Average Soil Properties of the Wüstebach Site Derived From 108 Soil Samples From 18 Locations Within the CRP Footprint, Collected According to the COSMOS Sampling Scheme

Depth (cm)	Organic Matter (%)	Organic Matter (kg/m^2)	Particle Density (g/cm^3)	Bulk Density (g/cm^3)	Porosity (%)	Lattice Water (kg/m^2)	Root Biomass (kg/m^2)
+5–0 (soil litter)	100	4.58	0.74	0.09	87.63		
0–5	31.65	6.20	2.05	0.39	80.84	0.51	1.000
5–10	11.95	3.90	2.42	0.65	73.04	1.29	0.774
10–15	8.16	3.39	2.49	0.83	66.69	1.90	0.599
15–20	4.32	2.17	2.57	1.01	60.79	2.44	0.463
20–25	3.03	1.56	2.59	1.03	60.33	2.35	0.358
25–30	2.78	1.57	2.60	1.13	56.58	2.54	0.277

$$z^* = 5.8\ (\theta_v + 0.0829)^{-1} \tag{6}$$

where θ_v is the volumetric soil water content (cm^3/cm^3). The additional hydrogen pools were considered by substituting θ_v with H_p:

$$z^* = 5.8\ \left(\rho_w^{-1} H_p + 0.0829\right)^{-1} \tag{7}$$

[22] Since the soils in the Wüstebach test site are relatively wet (>0.20 cm^3/cm^3), the effective measurement depth of the CRP will not exceed 30 cm. Table 1 lists the average soil properties of the Wüstebach site for these top 30 cm that were used to calculate the belowground hydrogen pools.

2.8. Determination of Hydrogen Pools Within the CRP Footprint

[23] Hydrogen present above the ground will affect the flux density of fast neutrons as measured by the CRP [*Zreda et al*., 2012]. In case of a forested catchment, some aboveground hydrogen pools are approximately static (e.g., biomass), but other hydrogen pools are expected to be more dynamic (interception of the forest canopy, water content of the litter layer, open water in river channels). To estimate hydrogen content of each pool, the moles of hydrogen were calculated from the mass of water.

[24] The dry biomass of the spruce forest in the Wüstebach test site was obtained from *Etmann* [2009] and converted to total dry mass in the footprint. Assuming a hydrogen content of 6% of the dry biomass [*Nurmi*, 1999] and an average timber water content of 65% by weight, the total hydrogen content of the spruce stand was estimated. For the estimation of hydrogen in the intercepted rainfall water in the forest canopy, we assumed an average instantaneous canopy storage capacity of 1.5 mm, which is a typical estimate for Norway spruce [*Rutter et al*., 1975].

[25] The hydrogen pool of the litter layer in spruce forest sites can account for a significant proportion of the total hydrogen in the footprint of the CRP [*Metzen*, 2012]. In addition, the water content of the litter layer can show a high temporal variability [*Schaap et al*., 1997]. Changing hydrogen content of such a dynamic pool is reflected in soil water content variations estimated by the CRP, which affects the measurement accuracy if not properly accounted for. It might even produce unrealistically high soil water content estimates that exceed the porosity of the soil. In the context of soil water content monitoring with CRP in forests, this effect needs to be considered. Unfortunately, no continuous measurements of water dynamics in the litter layer of the Wüstebach catchment are available for the study period. Therefore, we used a numerical solution of the 1-D Richards equation as implemented in the HYDRUS-1D software [*Simunek et al*., 2008] to simulate water dynamics in the litter layer. Soil hydraulic properties were parameterized using the Mualem-van Genuchten model:

$$\theta(h) = \begin{cases} \theta_r + \dfrac{\theta_s - \theta_r}{[1 + |\alpha h|^n]^m} & h < 0 \\ \theta_s & h \geq 0 \end{cases} \tag{8}$$

$$K(h) = K_s S_e^{0.5} \left[1 - \left(1 - S_e^{0.5/m}\right)^m\right]^2 \tag{9}$$

$$S_e = \frac{\theta - \theta_r}{\theta_s - \theta_r} \tag{10}$$

$$m = 1 - 1/n \qquad n > 1 \tag{11}$$

where h is the pressure head (cm), θ_r and θ_s are the residual and saturated water contents (cm^3/cm^3), α (1/cm) and n are empirical parameters which are, respectively, related to the air entry pressure value and the width of the pore size distribution, and K_s is the saturated hydraulic conductivity (cm/h). The Mualem-van Genuchten parameters θ_r, α, n, and K_s were inversely estimated from spatially averaged soil water contents at 5, 20, and 50 cm determined from the SoilNet sensors within the CRP footprint. This spatially averaged soil water content within the CRP footprint was obtained for each sensor depth using the procedure described in section 2.9. The soil profile in HYDRUS-1D was discretized into four materials (three soil horizons plus a litter layer of organic material on top of the soil) according to the layering of the typical soil profile (Figure 3). To estimate the hydraulic parameters of each soil layer, we used the global optimization scheme SCE-UA [*Duan et al*., 1992] and SoilNet data from 1 July 2009 to 31 December 2012. The root-mean-square error between measured and simulated water contents was selected as the objective function to be minimized. The value of θ_s was fixed to the maximum of the spatially averaged soil water content for each depth during the study period.

[26] Due to the lack of soil water content measurements in the litter layer, it was not possible to inversely estimate the hydraulic properties of the litter layer. The vegetation at the study site of *Schaap et al*. [1997] is similar to the Wüstebach site (about 50 year old homogenous coniferous forest). Because of the lack of better information, we assume

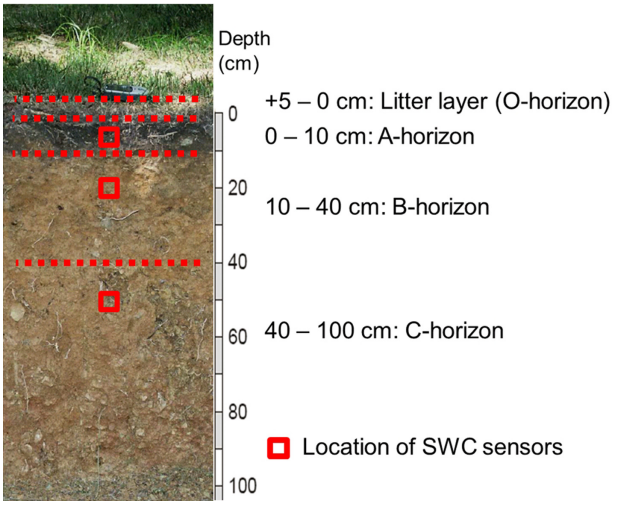

Figure 3. Typical soil profile at the Wüstebach test site and the vertical location of the in situ soil water content sensors.

that the hydraulic parameters of the litter layer determined by *Schaap et al*. [1997] are also valid for our study site. We only adapted the θ_s of the litter layer, which was estimated from the mean porosity of eight litter layer samples.

[27] Precipitation measured by the nearby weather station Kalterherberg was used as the top boundary condition in HYDRUS-1D. The reference potential evapotranspiration (ET_0) was computed with HYDRUS-1D using the Penman-Monteith equation [*Allen et al*., 1998] and meteorological data (global radiation, wind speed, relative humidity, and air temperature) from the same weather station. The potential transpiration (T) was calculated using leaf area index (LAI) and the radiation extinction coefficient (k) according to *Ritchie* [1972]:

$$T = ET_0\left(1 - e^{-k\times LAI}\right) \tag{12}$$

[28] We compared simulated with observed actual evapotranspiration rates from eddy covariance measurements within the Wüstebach catchment (data not shown) and achieved best correspondence using a k value of 0.75 and a LAI value of 4, which is within the range of typical LAI values for Norway spruce forests [*Pokorný and Stojnic*, 2012]. The root water uptake was computed by the Feddes approach [*Feddes et al*., 1976] implemented in HYDRUS-1D. The lower boundary condition of the HYDRUS-1D model was set to seepage face since the relatively thin soil layer overlays a fractured solid bedrock containing water conducting fissures [*Richter*, 2008]. The seepage face boundary condition assumes a no-flux boundary condition as long as the pressure head at the bottom of the soil profile is negative and a zero pressure head is used as soon as the bottom of the profile becomes saturated. We used this type of boundary condition to mimic drainage at the soil-bedrock interface. We assume that the bedrock is a significant flow barrier prohibiting drainage, but that fissures become preferential pathways for draining the soil profile once saturation is reached in the soil above the bedrock interface.

Table 2. Fitted Parameter of Equation (13) Describing Relationship Between the Cumulative Fraction of Counts and CRP Footprint Radius

Parameter	Fitted Values
a_1	6.32907E−13
a_2	6.40944E−10
a_3	2.51654E−07
a_4	5.25277E−05
a_5	8.01230E−03
a_6	6.79710E−04

2.9. Comparison of CRP With SoilNet

[29] To enable the comparison of the soil water content measurements from SoilNet with the CRP data, the in situ measurements of SoilNet need to be vertically and horizontally weighted to account for the instrument response of the CRP. In this study, we used empirical weighting functions that were developed on the basis of neutron transport simulation results using the MCNPx code [*Zreda et al*., 2008]. To obtain the horizontal weights, we fitted a polynomial function through the relationship between cumulative fraction of counts ($CFoC$) and CRP footprint radius (r) presented by *Zreda et al*. [2008]:

$$CFoC = a_1 r^5 + a_2 r^4 - a_3 r^3 + a_4 r^2 - a_5 r + a_6 \tag{13}$$

[30] The parameters a_1–a_6 are given in Table 2. The $CFoC$ for different CRP footprint radii calculated using equation (13) are provided in Table 3. In order to compensate for the uneven distribution of soil water content sensors in the CRP footprint, we divided the footprint area in circular segments with separations of 50 m. By assuming a maximum radius of 350 m, seven segments were obtained, and the horizontal weights w_h for each segment i were calculated using $w_{h,i} = CFoC_i - CFoC_{i-1}$. By subsequent rescaling, we ensured that the sum of $w_{h,i}$ equaled 1 for the seven segments (Table 3). Finally, the average soil water content within the CRP footprint was obtained using the average soil water content in each segment and the weights provided in Table 3.

[31] The in situ soil moisture sensors only covered about 66% of the CRP footprint (see Figure 1). However, the sensitivity of the cosmic-ray sensor decreases with distance as outlined above. The area which is not covered by SoilNet has an average distance to the cosmic-ray sensor of 250 m. Using equation (13), we calculated a $CFoC$ of 0.77 for a

Table 3. $CFoC$ Values for Different Radii and Horizontal Weights (w_h) for Seven Radial Segments Used for the Comparison of the Soil Water Content Measurements From SoilNet With the CRP Data

Footprint Radius (m)	CFoC	Segment	w_h
0	0		
50	0.298	0–50	0.344
100	0.471	50–100	0.200
150	0.594	100–150	0.142
200	0.692	150–200	0.114
250	0.767	200–250	0.087
300	0.818	250–300	0.058
350	0.866	300–350	0.056

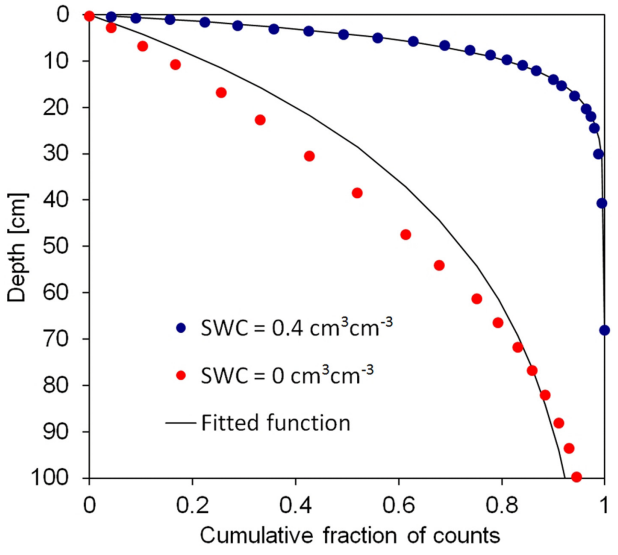

Figure 4. Cumulative fraction of counts as a function of depth obtained from *Zreda et al*. [2008]. The fitted empirical model (equation (17)) is also shown. The values for γ were 39 for a soil water content of 0.40 cm^3/cm^3 and 6 for a soil water content of 0 cm^3/cm^3, respectively.

distance of 250 m. In other words, more than 77% neutron counts observed with the CRP originated from the area covered by SoilNet. In addition, the land use and soil types are similar in the surrounding area. Therefore, we are confident that the spatially averaged soil water content is representative for the CRP footprint.

[32] Since the sensor depth of the CRP is strongly dependent on soil water content, a more complex procedure is necessary to obtain the vertical weights that are required to compare the in situ water content data with the cosmic-ray data. We selected an empirical function to describe the relationship between *CFoC* and depth (z) published by *Zreda et al*. [2008] for two soil water contents:

$$z = -\gamma \cdot \ln(1 - CFoC) \tag{14}$$

[33] The empirical functions fitted to the data of *Zreda et al*. [2008] are shown in Figure 4. The function was able to fit the wet case very well (RMSE: 0.3 cm), whereas the dry case resulted in a less reliable fit (RMSE: 5.9 cm). However, since the lowest observed mean soil water content at the Wüstebach site was 0.24 cm^3/cm^3, we do not expect this uncertainty to produce large errors in the estimates of vertical weights.

[34] For the application of equation (14), the parameter γ needs to be related to the soil water content. According to *Franz et al*. [2012a], the two e-folding sampling volume is defined as the volume within which 86% of the detected neutrons above the surface originate. Therefore, the effective depth of the cosmic-ray probe z^* is defined as the 86% cumulative sensitivity point:

$$z^* = -\gamma \cdot \ln(1 - 0.86) \tag{15}$$

[35] Combining equations (7) and (15) yields a direct relationship between γ and the total amount of hydrogen present in the soil within the effective CRP sensor depth including the litter layer:

$$\gamma = \frac{-5.8}{\ln(0.14) \cdot (H_p + 0.0829)} \tag{16}$$

[36] By rearranging equation (14), *CFoC* for a sensor at depth z can be calculated as follows:

$$CFoC_z = 1 - e^{\left(-\frac{z}{\gamma}\right)} \tag{17}$$

[37] We used an iterative calculation procedure to derive vertical weights for each sensor depth. First, the vertical average of the measured soil water content profile was used to obtain an approximate estimate of γ, which is then used to calculate *CFoC* for the upper sensor (in our case at 5 cm). The vertical weight at 5 cm is obtained with $w_{z,\ 5cm} = CFoC_{5cm}$. For the next sensor depth (in our case at 20 cm), the vertical weight is calculated with $w_{z,\ 20cm} = CFoC_{20cm} - CFoC_{5cm}$. The deepest location (in our case at 50 cm) contributed the remaining weight toward 100% of the cumulative fraction of counts. Using these weights, a new estimate of the weighted average soil water content was calculated, and this procedure was repeated until the change in updated weighted average water content was negligible (<0.0001 cm^3/cm^3). Typically, five iterations were sufficient. *Franz et al*. [2012b] presented a simpler (linear) approach for the vertical weighing of in situ measurements. However, this simple approach neglects the inherent nonlinear averaging of the CRP probe with depth (Figure 4). In future work, the validity and accuracy of both approaches should be compared.

3. Results and Discussion

3.1. Characterization of Hydrogen Pools Within the CRP Footprint

[38] The estimated distribution of the hydrogen pools for the Wüstebach catchment is shown in Figure 5. The amount of hydrogen in each pool was calculated for three cases: wet (highest measured soil water content, high simulated water content of the litter layer, full interception storage), average (average soil water content, average water content of the litter layer, no interception), and dry conditions (lowest measured soil water content, lowest simulated water content of the litter layer, no interception). Independent of catchment wetness, more than half of the hydrogen is present as soil water, interception in the forest floor, and additional belowground hydrogen pools. Under dry conditions, soil water accounts for 31.4% of the hydrogen, whereas under wet conditions the contribution of intercepted water (36%) in the litter layer exceeds the contribution of soil water (21.1%). The reason for the low contribution of soil water is the shallow measurement depth during wet conditions (<0.1 m, see section 3.2). This highlights that the water dynamics of the forest floor of the Wüstebach catchment need to be accounted for in the interpretation of the CRP measurements.

[39] The static belowground hydrogen pools (lattice water, organic matter, and root biomass) accounted for only 2.3% of the total hydrogen content under wet

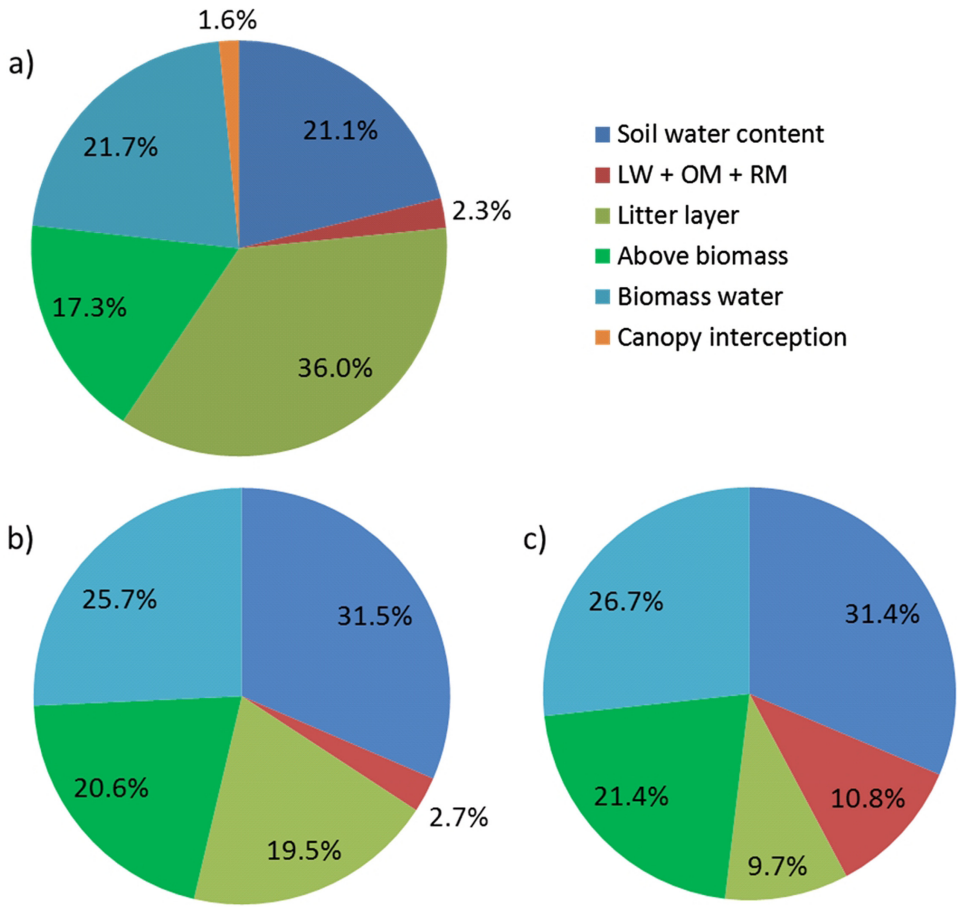

Figure 5. Estimated percentages of hydrogen in the main hydrogen pools present within the footprint of the CRP in the Wüstebach site for different catchment wetness conditions during the study period: (a) maximal wetness, (b) average wetness, and (c) driest condition (OM, organic matter; LW, lattice water; RM, root biomass).

conditions and the contribution increased up to 10.8% under dry conditions. Hydrogen stored in the trees as carbohydrates and in tissue water accounts for approximately 39–48% of the hydrogen pool. Assuming a mean instantaneous interception storage capacity of 1.5 mm, canopy interception makes up ~1.6% of the total hydrogen content in the CRP footprint. According to *Klaassen et al.* [1998], the storage capacity of coniferous trees does not exceed 3 mm, which would lead to a maximum contribution of ~3.1% of the total hydrogen in the CRP footprint. Therefore, we neglected the contribution of the dynamic aboveground hydrogen pool associated with canopy interception. The static aboveground hydrogen pools affect the incoming neutron flux, and we assumed here that this can be accounted for by calibration of N_0 against in situ soil water content measurements.

3.2. Effective Sensor Depth

[40] Figure 6 illustrates how the effective sensor depth (z^*) decreases with increasing soil water content and increasing number of belowground hydrogen pools. For dry conditions, z^* is approximately 70 cm without considering additional hydrogen pools and less than 40 cm for the case that all belowground hydrogen pools are included. Due to the high amount of organic matter in the litter layer and in

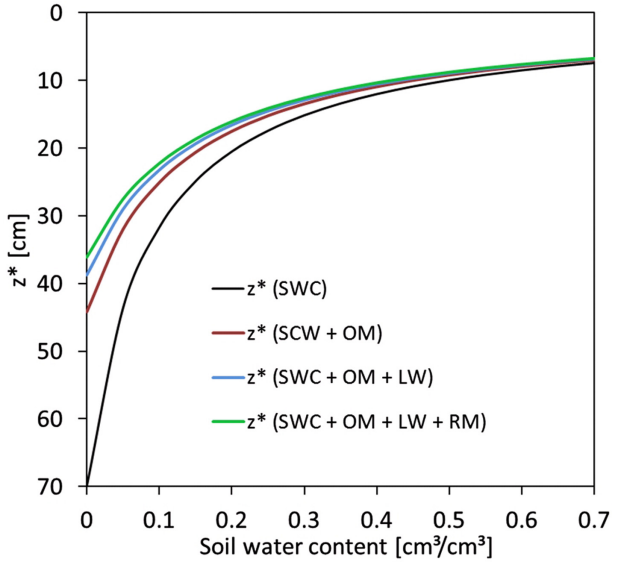

Figure 6. The effective sensor depth versus soil water content for different hydrogen pool combinations (SWC, soil water content; OM, organic matter; LW, lattice water; RM, root biomass), including the litter layer.

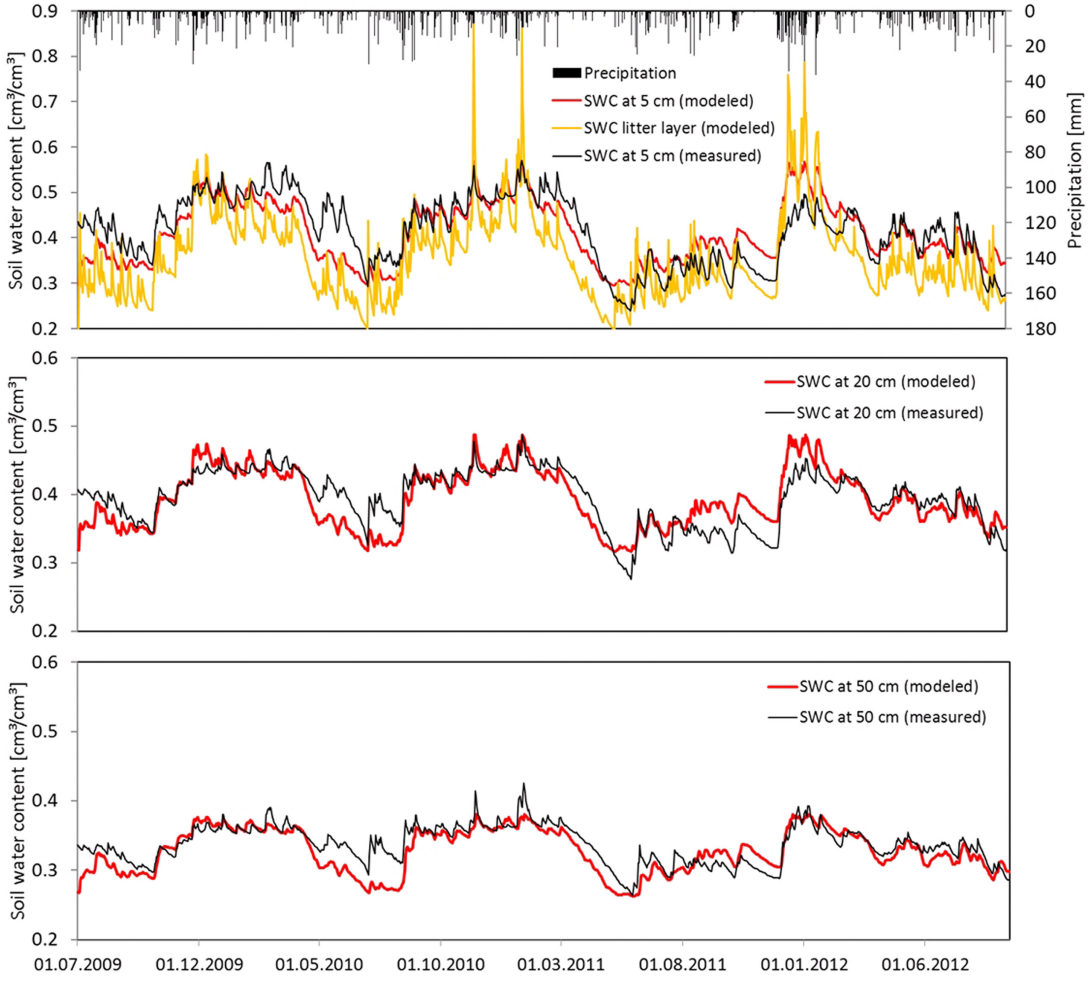

Figure 7. Observed versus simulated soil water contents in 5, 20, and 50 cm depth as well as the simulated water dynamics of the litter layer using the inverse HYDRUS-1D model.

the top layer of the mineral soil of the Wüstebach catchment (see Table 1), the amount of hydrogen present in this compartment is relatively high and corresponds to an average soil water content equivalent of 0.048 m^3/m^3 in the top 0.15 m. The hydrogen located in lattice water and root biomass is considerably lower (the soil water content equivalent being 0.012 and 0.015 m^3/m^3, respectively). For this reason, organic matter is the most important hydrogen pool beside soil water in reducing the CRP sensing depth in this catchment. For driest conditions (average soil water content: ~0.2 cm^3/cm^3), it reduced the sensing depths by about 15%, whereas lattice water and root biomass reduced the sensing depth by 2.9% and 4.0%, respectively. In the case of wetter soil conditions, the effect of additional hydrogen pools decreased significantly, so that for very wet soil conditions (e.g., 0.7 cm^3/cm^3) the difference is negligible. We believe that these results are representative for similar forest ecosystems with a significant litter layer.

3.3. Modeled Water Dynamics of the Litter Layer

[41] Figure 7 shows the observed and simulated soil water contents in 5, 20, and 50 cm depth as well as the simulated water dynamics of the litter layer, and Figure 8 presents the soil water retention and hydraulic conductivity functions obtained using inverse modeling of the Mualem-van Genuchten parameters (Table 4). The HYDRUS-1D model with optimized hydraulic parameters was able to reproduce the soil water contents dynamics at 5, 20, and 50 cm depth reasonably well (RMSE were 0.036, 0.020, and 0.015 cm^3/cm^3, respectively). The highest deviation between measured and simulated soil water contents occurred during drying periods indicating an overestimation of evapotranspiration during these periods. As expected, the water content of the litter layer showed higher temporal dynamics than the soil water content in 5 cm, which is mainly a result of the high porosity (see Table 4). From Figure 8 and Table 4, it can be seen that the parameter θ_s decreased with depth, which reflects the increasing soil compaction with depth. Interestingly, the Bv-Sw-horizon shows a distinctly higher saturated hydraulic conductivity compared to the other horizons. This corresponds well with the typical hydraulic characteristics of planosol soils featuring a highly permeable E-horizon above a less permeable B-horizon. These examples demonstrate that the inverse HYDRUS-1D model application produced plausible soil hydraulic parameters. Although we do not have data to validate the simulated water dynamics in the litter layer, we consider the simulation to be accurate enough to analyze the effect of the litter layer on the neutron count rate.

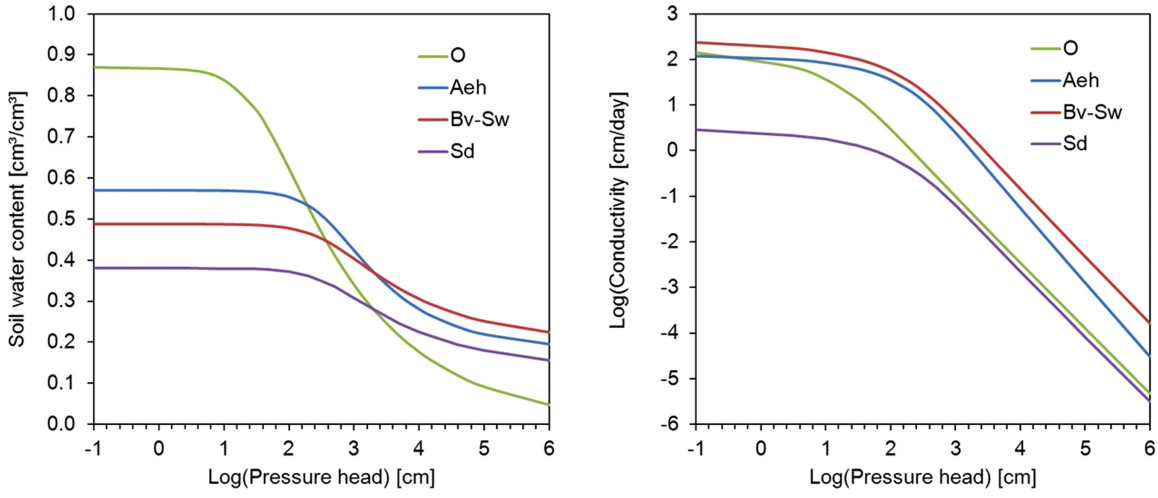

Figure 8. (left) Soil water retention and (right) hydraulic conductivity functions as given by equations (8) and (9), respectively, according to the soil hydraulic properties given in Table 4.

3.4. Uncertainty of CRP Data

[42] Figure 9 shows neutron count rates of the Wüstebach site corrected for atmospheric pressure, air humidity, and incoming neutrons for different temporal resolutions (original hourly data as well as 12 and 24 h running averages) during the study period. It is evident that averaging removed high-frequency noise that we attribute to uncertainty in the count rate. In order to identify the most appropriate temporal resolution for soil water content determination, we used a synthetic Monte Carlo uncertainty analysis. Neutron measurements are governed by Poissonian statistics, and thus, the standard deviation σ_X associated with a neutron count X is $X^{0.5}$. The standard deviation associated with different time resolutions can be calculated using

$$\sigma_X = X^{0.5} = (aN)^{0.5} \tag{18}$$

where a is the length of the interval (h) and N is the amount of counts per hour. We created large sets of random draws from Poisson distributions with mean values of N ranging from 650 to 1200 counts/h and different values of a. This range of N values was chosen to represent different wetness conditions of the Wüstebach site corresponding to average soil water contents between 0.1 and 0.7 cm^3/cm^3. The uncorrected N values were used because they represent the actual neutron count measurement uncertainty (e.g., due to the pressure correction procedure N values are scaled to sea level). In a next step, corrections were applied to the simulated neutron counts using equations (1)–(3), and soil water content was obtained using equation (4) and a bulk density of 1.0 g/cm^3. The standard deviation of the soil water content σ_θ thus obtained is presented in Figure 10. As expected, σ_θ is strongly dependent on the temporal resolution, but also on the average soil water content. For hourly data, σ_θ is 0.013 cm^3/cm^3 for a soil water content of 0.1 cm^3/cm^3 and 0.183 cm^3/cm^3 for a soil water content of 0.7 cm^3/cm^3. Clearly, the hourly neutron count rates at the Wüstebach site are too low for accurate soil water content determination with an hourly resolution. With longer integration times, σ_θ significantly decreases and is below 0.04 cm^3/cm^3 for 12 h data and below 0.03 cm^3/cm^3 for 24 h data even in the case of an exceptionally high soil water content of 0.70 cm^3/cm^3. As a trade-off between uncertainty and time resolution, we decided to use 24 h averages of N.

3.5. Calibration of the CRP Using In Situ SoilNet Data

[43] We used the weighted average soil water content data from SoilNet to calibrate the CRP measurements (equation (4)) for the estimation of soil water content from the measured fast neutron count rates. As suggested by *Desilets et al*. [2010], we only calibrated the N_0 parameter. We used the average bulk density of the top 30 cm (0.84 g/cm^3) as suggested by *Franz et al*. [2012b] to convert the gravimetric water content to the volumetric water content. Clearly, the use of the average bulk density neglects the variation in CRP sensing depth. Given the low bulk density in the top soil, this simplification may lead to additional uncertainty in volumetric soil water content estimation, especially during very wet conditions (sensing depth <15 cm). We suggest that this problem should be investigated in more detail in future studies on CRP calibration.

[44] The results of different calibration options are listed in Table 5. When using the uncorrected fast neutron count data, the RMSE for the whole period is large (almost 0.1 cm^3/cm^3). It reduces significantly after all corrections (atmospheric pressure, humidity, and incoming neutrons correction) have been applied (0.030 cm^3/cm^3, see also Figures 11 and 13). However, still some larger deviations

Table 4. Optimized Soil Hydraulic Properties, Parameters of *Schaap et al*. [1997] (Underlined Letters), and Measured Saturated Water Content (Bold Letters)

Soil Horizon	n	α	θ_r	θ_s	K_s (cm/h)
O	<u>1.286</u>	<u>0.0264</u>	<u>0</u>	**0.870**	<u>200.0</u>
A	<u>1.411</u>	<u>0.00268</u>	<u>0</u>.180	0.570	<u>125.5</u>
E	1.305	0.00253	0.198	0.488	271.9
B	1.322	0.00105	0.134	0.380	3.24

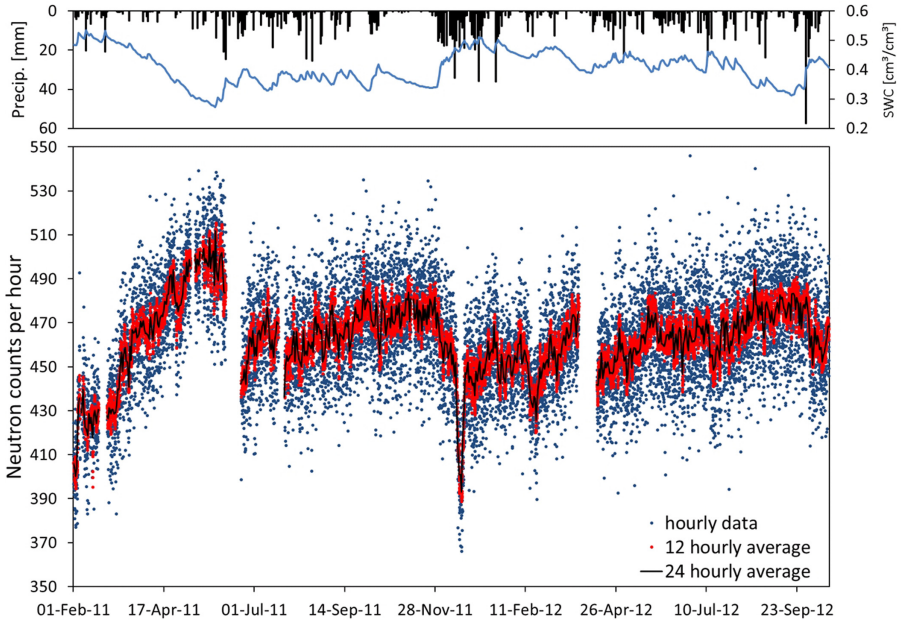

Figure 9. (top) Daily precipitation from the meteorological station Kalterherberg as well as vertically and horizontally weighted averages of daily in situ soil water content and (bottom) time series of corrected neutron count rates measured at the Wüstebach site (original hourly data as well as 12 and 24 hourly averages).

between the two water content time series are apparent in Figure 11. In particular, a significant overestimation of water content is visible during 4 days in December 2011 and December 2012. During these days with snow, the estimated soil water content exceeded the expected values by more than 0.5 cm^3/cm^3. This can be attributed to thick snow covers, which depressed the fast neutron intensity. Since the amount of slow neutrons increases when snow is present, *Desilets et al*. [2010] suggested that this effect can potentially be used to estimate the snow cover depth from CRP measurements. However, since an appropriate method is still not available, more research is needed to come up with appropriate estimates of average snow depths from CRP data. In order to avoid propagating erroneous measurements affected by snow into the calibration, we excluded time periods with snow from the calibration.

[45] *Zreda et al*. [2012] argued that it is important to consider belowground hydrogen pools for soil water content determination from CRP measurements. In order to test whether consideration of belowground hydrogen pools (lattice water, organic matter, litter layer, and root biomass) is also important in ecosystems with litter layer, we compared different calibration options: (3) including only the static belowground hydrogen pools, (4) including only water dynamics of the litter layer, and (5) including both static belowground hydrogen pools and water dynamics of the litter layer. The consideration of belowground hydrogen pools led to a decrease in the accuracy of soil water content determination in this study (see options 3 and 5). This is the first study that compared the accuracy of soil water content determination with and without corrections for belowground hydrogen pools, and it is not clear at this point whether the decrease in accuracy is systemic or only occurs for our study site. If one considers that accounting for belowground pools effectively leads to lower neutron counts and thus steeper calibration curves, it seems not surprising that a decrease of accuracy was observed for the humid Wüstebach test site. Three other explanations for the decrease in accuracy when considering belowground hydrogen pools are related to (i) the uncertainty in determining lattice water, soil organic matter, and root biomass in the face of spatial variability of these properties, (ii) the uncertainty in effective measurement depth through uncertain belowground hydrogen pools, and (iii) the shallow measurement depth of the CRP measurement in relation to the sensor positions of the SoilNet. Clearly, more research

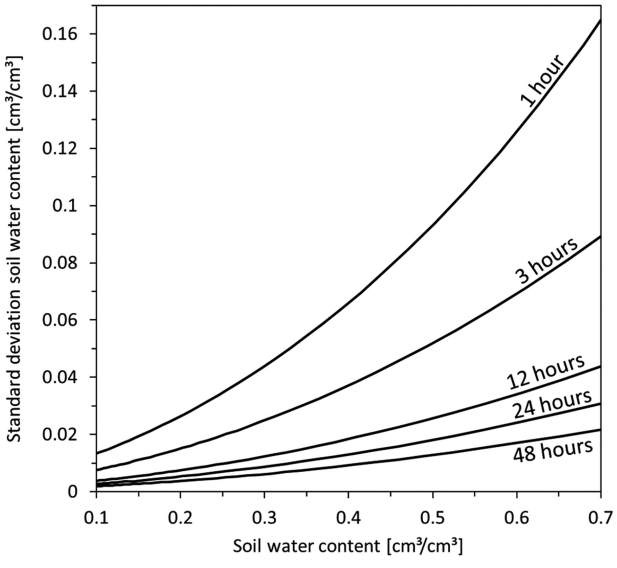

Figure 10. Standard deviation of soil water content determined by a cosmic-ray probe versus mean soil water content for different neutron count integration times.

Table 5. Calibration Results of Different Options[a]

Option[b]	N_o	Mean SWC (neutron counts) (cm^3/cm^3)	Mean SWC (SoilNet) (cm^3/cm^3)	Difference in mean SWC (%)	RMSE (cm^3/cm^3)	RMSE 2011 (cm^3/cm^3)	RMSE 2012 (cm^3/cm^3)
1	1397.7	0.380	0.405	−6.327	0.0918	0.0771	0.1034
2	919.8	0.404	0.405	−0.216	0.0304	0.0318	0.0294
3	940.6	0.404	0.405	−0.215	0.0333	0.0351	0.0319
4	913.1	0.391	0.392	−0.189	**0.0294**	**0.0274**	0.0310
5	934.8	0.391	0.392	−0.039	0.0309	0.0289	0.0325

[a]Bold characters indicate lowest values of the objective criteria.
[b]Calibration using uncorrected fast neutron counts. Calibration using corrected fast neutron counts (atmospheric pressure, air humidity, and incoming radiation correction). Calibration using corrected fast neutron counts (see option 2) including belowground hydrogen pools. Calibration using corrected fast neutron counts (see option 2) including water dynamics of the litter layer. Calibration using corrected fast neutron counts (see option 2) including belowground hydrogen pools and water dynamics of the litter layer.

is required to establish adequate procedures to account for belowground hydrogen pools and to validate CRP measurements for soil water content determination in general.

[46] In a next step, we considered the simulated water content of the litter layer in the soil water content determination with the CRP. The result of this calibration is presented in Figures 12 and 13 (right). The new calibration resulted in a RMSE of 0.0294 cm^3/cm^3 for the whole period (see option 4 in Table 5). Especially for 2011, a better correspondence with the SoilNet data was obtained by including the dynamics of the litter layer. The RMSE was 0.0274 cm^3/cm^3 compared to 0.0318 cm^3/cm^3 when the litter layer was not considered. This indicates that water dynamics of the litter layer affect the fast neutron emission and thus should preferably be considered in the calibration when CRPs are used in forest ecosystems with a significant litter layer. On the other hand, consideration of the litter layer resulted in an increase of the RMSE for 2012, indicating that the water dynamics of the litter layer are not well enough represented. This is especially true for the particularly wet and cold period from January to April 2012, in which the RMSE increased from 0.0435 to 0.0501 cm^3/cm^3 when the litter was considered. The reason for this discrepancy is an overestimation of water content in the litter layer during this time period, which is attributed to the considerable uncertainty in the soil hydraulic parameters for the litter layer (for instance, the porosity of the litter layer may be too high). Therefore, future studies should consider the direct measurement of the water dynamics in the litter layer to enable a better interpretation of cosmic-ray data from humid forest ecosystems.

4. Conclusions

[47] We investigated the accuracy of CRP measurements for soil water content determination in a humid forested catchment with a litter layer. The high amount of hydrogen located in pools other than soil water can potentially reduce the accuracy of soil water content determination with the CRP, which makes this evaluation a worst case scenario. We used soil water content data from a wireless soil water content sensor network to calibrate the cosmic-ray sensor and to determine the accuracy of soil water content determination.

[48] The significant amount of lattice water and carbohydrates in soil organic matter and belowground biomass in the soil of the Wüstebach catchment reduced the effective

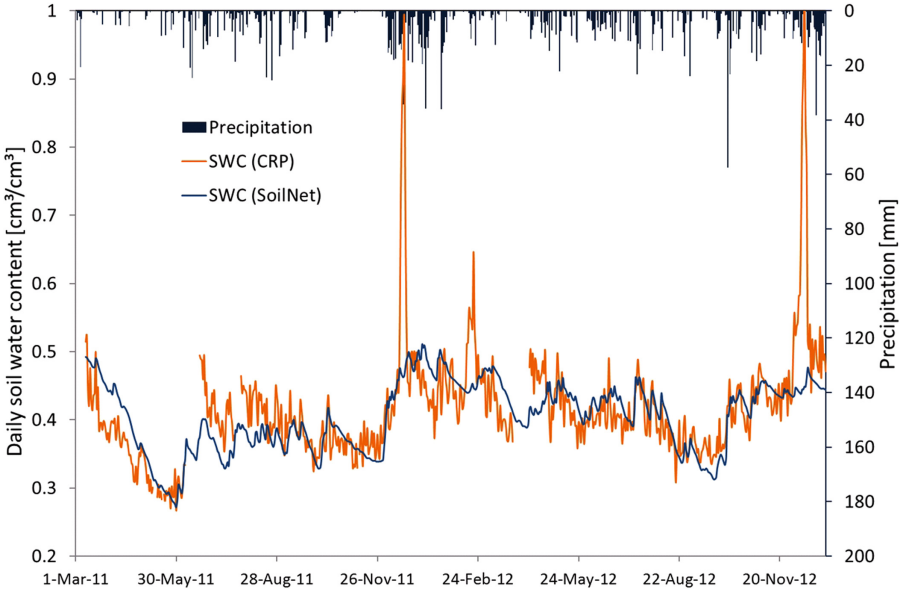

Figure 11. Time series of weighted average soil water content (SoilNet) and soil water content derived from fast neutron count rates using calibration option 2 (see Table 5).

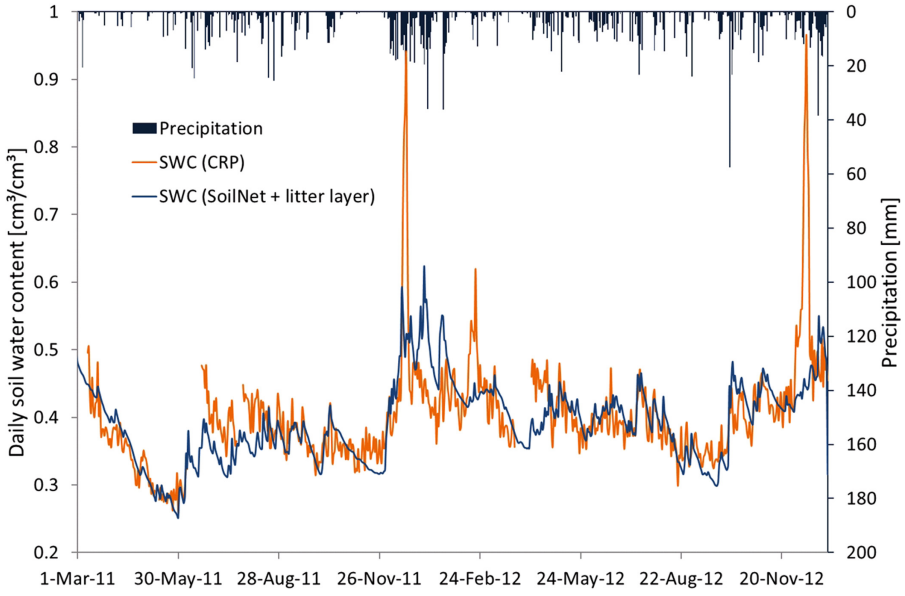

Figure 12. Time series of weighted average soil water content (SoilNet) and soil water content derived from fast neutron count rates using calibration option 4 (see Table 5) that considers simulated water dynamics of the litter layer.

sensor depth especially during dry conditions, in which the sensor depth was reduced by up to 50%. Therefore, we suggest that the belowground hydrogen pools need to be accounted for in similar forest ecosystem in order to determine the effective sensor depth.

[49] A synthetic uncertainty analysis showed that the neutron count integration time has a strong effect on the accuracy of soil water content determination using CRP. Short time intervals will significantly increase the measurement uncertainty for sites with low neutron count rate levels. This is very important in humid forest ecosystems like the Wüstebach catchment, which is located at a relatively low altitude and has a large amount of hydrogen located in aboveground and belowground hydrogen pools. These factors contribute to reduced count rates and thus decrease the sensitivity of the CRP. Therefore, a 24 h integration time was chosen as a trade-off between uncertainty and time resolution for the Wüstebach catchment. In order to reliably measure with a higher temporal resolution in humid forest ecosystems, a CRP with multiple detector tubes is needed. For instance, to achieve a six hourly resolution with the same accuracy achieved here, four standard CRP detector tubes would be needed.

[50] A further component that complicates the application of CRP in humid forest ecosystems is the water content dynamics of the litter layer. We found that including simulated water contents of the litter layer in the calibration provided slightly better calibration results (RMSE of 0.029 cm^3/cm^3) and thus should be considered in the calibration when CRP measurements are used for soil water content

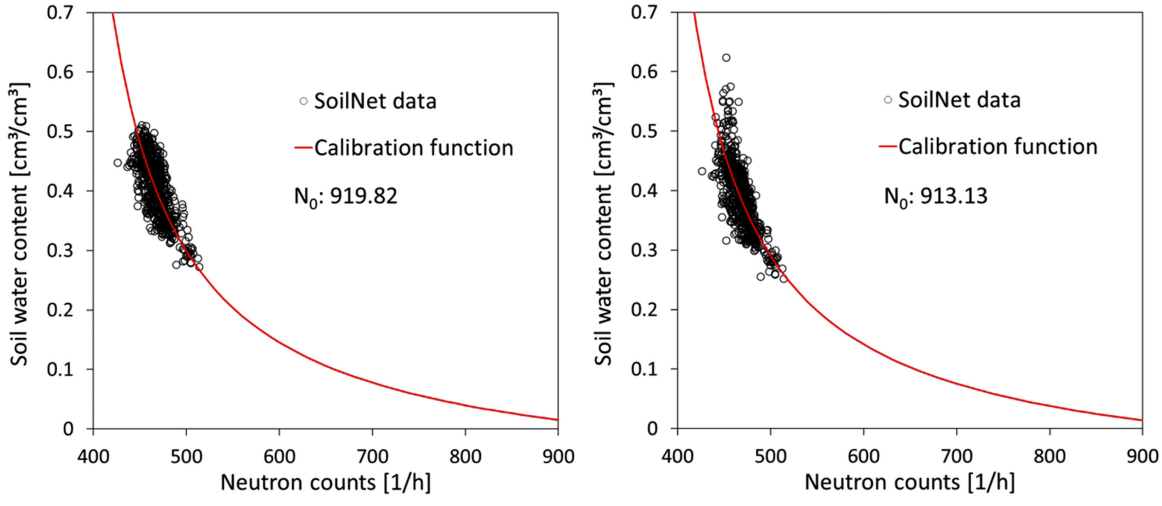

Figure 13. Relationship between daily observed fast neutron counts and daily weighted average soil water contents from SoilNet (left) without and (right) with consideration of litter layer water dynamics as well as the associated calibration functions.

estimation in forest ecosystems with a significant litter layer. However, without considering explicitly the litter layer, the CRP allowed the assessment of integral daily soil water content dynamics with a RMSE smaller than 0.04 cm^3/cm^3 for the Wüstebach catchment.

[51] Although previous studies stated that belowground hydrogen pools should be considered in the calibration of CRP, this led to a decrease in the accuracy of soil water content determination for the Wüstebach catchment. This discrepancy is most likely related to uncertainties in the data used for correction and in the calibration procedure itself. Therefore, we suggest additional research to establish adequate procedures to account for additional hydrogen pools as well as for the effects of temporal changes in hydrogen pools (e.g., biomass in crops) to decrease the uncertainty in soil water content determination using cosmic-ray neutrons in humid forest ecosystems.

[52] **Acknowledgments.** We gratefully acknowledge the support by the SFB-TR32 "Pattern in Soil-Vegetation-Atmosphere Systems: Monitoring, Modelling and Data Assimilation" funded by the Deutsche Forschungsgemeinschaft (DFG), TERENO (Terrestrial Environmental Observatories) funded by the Helmholtz-Gemeinschaft, and ExpeER funded by EU-FP7. We also acknowledge the NMDB database funded by EU-FP7 and the German weather service for providing data. Daniel Metzen and Daniel Dolfus are thanked for supporting the setup and ongoing maintenance of the CRP. Trenton Franz and Marek Zreda are thanked for fruitful discussions. Finally, the three reviewers and the Associate Editor are thanked for their constructive comments that significantly improved this manuscript.

References

Allen, R. G., L. S. Pereira, D. Raes, and M. Smith (1998), Crop evapotranspiration—Guidelines for computing crop water requirements, FAO Irrig. and Drain. Pap. 56, Nat. Resour. Manage., Rome.

Bogena, H. R., M. Herbst, J. A. Huisman, U. Rosenbaum, A. Weuthen, and H. Vereecken (2010), Potential of wireless sensor networks for measuring soil water content variability, *Vadose Zone J.*, *9*(4), 1002–1013, doi:10.2136/vzj2009.0173.

Desilets, D., and M. Zreda (2001), On scaling cosmogenic nuclide production rates for altitude and latitude using cosmic-ray measurements, *Earth Planet. Sci. Lett.*, *193*, 213–225.

Desilets, D., and M. Zreda (2003), Spatial and temporal distribution of secondary cosmic-ray nucleon intensities and applications to in-situ cosmogenic dating, *Earth Planet. Sci. Lett.*, *206*, 21–42.

Desilets, D., and M. Zreda (2013), Footprint diameter for a cosmic-ray soil moisture probe: Theory and Monte Carlo simulations, *Water Resour. Res.*, *49*, 3566–3575, doi:10.1002/wrcr.20187.

Desilets, D., M. Zreda, and T. P. A. Ferre (2010), Nature's neutron probe: Land surface hydrology at an elusive scale with cosmic rays, *Water Resour. Res.*, *46*, W11505, doi:10.1029/2009WR008726.

Duan, Q., S. Sorooshian, and V. Gupta (1992), Effective and efficient global optimization for conceptiual rainfall-runoff models, *Water Resour. Res.*, *28*(4), 1015–1031, doi:10.1029/91WR02985.

Etmann, M. (2009), *Dendrologische Aufnahmen im Wassereinzugsgebiet Oberer Wüstebach anhand verschiedener Mess- und Schätzverfahren*, Master thesis, 80 pp., Univ. of Münster.

Feddes, R. A., P. Kowalik, K. Kolinskamalinka, and H. Zaradny (1976), Simulation of field water-uptake by plants using a soil-water dependent root extraction function, *J. Hydrol.*, *31*, 13–26.

Franz, T. E., M. Zreda, T. P. A. Ferre, R. Rosolem, C. Zweck, S. Stillman, X. Zeng, and W. J. Shuttleworth (2012a), Measurement depth of the cosmic-ray soil moisture probe affected by hydrogen from various sources, *Water Resour. Res.*, *48*, W08515, doi:10.1029/2012WR011871.

Franz, T. E., M. Zreda, R., Rosolem, and P. A. Ferre (2012b), Field validation of cosmic-ray soil moisture sensor using a distributed sensor network, *Vadose Zone J.*, *11*, doi:10.2136/vzj2012.0046.

Franz, T. E., M. Zreda, R. Rosolem, and T. P. A. Ferre (2013), A universal calibration function for determination of soil moisture with cosmic-ray neutrons, *Hydrol. Earth Syst. Sci.*, *17*, 453–460, doi:10.5194/hess-17–453-2013.

Gaisser, T. K. (1990), *Cosmic Rays and Particle Physics*, Cambridge Univ. Press, Cambridge, U. K.

Gregory, P. J. (2006), Roots, rhizosphere and soil: The route to a better understanding of soil science?, *Eur. J. Soil Sci.*, *57*, 2–12, doi:10.1111/j.1365–2389.2005.00778.

Hendrick, L. D., and R. D. Edge (1966), Cosmic-ray neutrons near the earth, *Phys. Rev.*, *145*, 1023–1025.

Hess, W. N., E. H. Canfield, and R. E. Lingenfelter (1961), Cosmic-ray neutron demography, *J. Geophys. Res.*, *66*, 665–677, doi:10.1029/JZ066i003p00665.

Klaassen, W., F. Bosveld, and E. De Water (1998), Water storage and evaporation as constituents of rainfall interception, *J. Hydrol.*, *212–213*, 36–50.

Lal, D., and B. Peters (1967), Cosmic-ray produced radioactivity on the earth, in *Handbuch der Physik*, edited by K. Sitte, pp. 551–612, Springer, Berlin.

Metzen, D. (2012), *Capability of the cosmic-ray sensor for the assessment of mesoscale soil moisture variability in the catchment of the Rur River*, Master thesis, 80 pp., Geogr. Inst. der Rheinischen Friedrich-Wilhelms-Univ. Bonn.

Nurmi, J. (1999), The storage of logging residue for fuel, *Biomass Bioenergy*, *17*(1), 41–47.

Parker, E. N. (1965), The passage of energetic charged particles through interplanetary space, *Planet. Space Sci.*, *13*, 9–49.

Phillips, F. M., W. D. Stone, and J. T. Fabryka-Martin (2001), An improved approach to calculating low-energy cosmic-ray neutron fluxes near the land/atmosphere interface, *Chem. Geol.*, *175*, 689–701.

Pokorný, R., and S. Stojnic (2012), Leaf area index of Norway spruce stands in relation to age and defoliation, *Beskydy*, *5*(2), 173–180.

Richter, F. (2008), *Bodenkarte zur Standorterkundung. Verfahren Quellgebiet Wüstebachtal (Forst)*, Geol. Dienst Nordrhein-Westfalen, Krefeld, Germany.

Ritchie, J. T. (1972), Model for predicting evaporation from a row crop with incomplete cover, *Water Resour. Res.*, *8*(5), 1204–1213, doi:10.1029/WR008i005p01204.

Rivera Villarreyes, C. A., G. Baroni, and S. E. Oswald (2011), Integral quantification of seasonal soil moisture changes in farmland by cosmic-ray neurons, *Hydrol. Earth Syst. Sci.*, *15*, 3843–3859.

Rosenbaum, U., J. A. Huisman, A. Weuthen, H. Vereecken, and H. R. Bogena (2010), Sensor-to-sensor variability of the ECH2O EC-5, TE, and 5TE sensors in dielectric liquids, *Vadose Zone J.*, *9*, 181–186, doi:10.2136/vzj2009.0036.

Rosenbaum, U., H. R. Bogena, M. Herbst, J. A. Huisman, T. J. Peterson, A. Weuthen, A. W. Western, and H. Vereecken (2012), Seasonal and event dynamics of spatial soil moisture patterns at the small catchment scale, *Water Resour. Res.*, *48*, W10544, doi:10.1029/2011WR011518.

Rosolem, R., W. J. Shuttleworth, M. Zreda, T. E. Franz, X. Zeng, and S. A. Kurc (2013), The effect of atmospheric water vapor on the cosmic-ray soil moisture signal, *J. Hydrometeorol.*, doi:10.1175/JHM-D-12–0120.1.

Rutter, A. J., A. J. Morton, and P. C. Robins (1975), A predictive model of rainfall interception in forests. II Generalization of the model and comparison with observations in some coniferous and hardwood stands, *J. Appl. Ecol.*, *12*, 367–380.

Schaap, M. P., W. Bouten, and J. M. Verstraten (1997), Forrest floor water content dynamics in a Douglas fir stand, *J. Hydrol.*, *201*, 367–383.

Simunek, J., M. T. van Genuchten, and M. Sejna (2008), Development and applications of the HYDRUS and STANMOD software packages and related codes, *Vadose Zone J.*, *7*(2), 587–600, doi:10.2136/Vzj2007.0077.

Vereecken, H., J. A. Huisman, H. R. Bogena, J. Vanderborght, J. A. Vrugt, and J. W. Hopmans (2008), On the value of soil moisture measurements in vadose zone hydrology. A review, *Water Resour. Res.*, *44*, W00D06, doi:10.1029/2008WR006829.

Zacharias, S., et al. (2011), A network of terrestrial environmental observatories in Germany, *Vadose Zone J.*, *10*, 955–973, doi:10.2136/vzj2010.0139.

Zreda, M., D. Desilets, T. P. A. Ferré, and R. L. Scott (2008), Measuring soil moisture content non-invasively at intermediate spatial scale using cosmic-ray neutrons, *Geophys. Res. Lett.*, *35*, L21402, doi:10.1029/2008GL035655.

Zreda, M., W. J. Shuttleworth, X. Xeng, C. Zweck, D. Desilets, T. E. Franz, R. Rosolem, and P. A. Ferre (2012), COSMOS: The COsmic-ray Soil Moisture Observing System, *Hydrol. Earth Syst. Sci.*, *16*, 4079–4099, doi:10.5194/hess-16-1-2012.